Annealing-induced crystalline structure and mechanical property changes of polypropylene random copolymer

Jing-wei Chen, Jian Dai, Jing-hui Yang, Ting Huang, Nan Zhang, and Yong Wang[a)]
Key Laboratory of Advanced Technologies of Materials (Ministry of Education), School of Materials Science and Engineering, Southwest Jiaotong University, Chengdu 610031, China

(Received 13 August 2013; accepted 25 September 2013)

In this work, the effects of annealing treatment on the crystalline structure and mechanical property changes of polypropylene random copolymer (PPR) were comparatively investigated. Wide angle x-ray diffraction and differential scanning calorimetry were used to study the crystalline structure evolution of the annealed PPR sample. The relaxation behavior of the annealed PPR sample was analyzed using dynamic mechanical analysis. The mechanical properties and the toughening mechanism were also investigated. The results showed that the crystalline structure evolution of the annealed PPR sample depended on the annealing temperature. Due to the largely increased molecular chain mobility in the amorphous region, which promoted the plastic deformation of the annealed PPR sample under the impact condition, largely enhanced impact strength was achieved at a moderate annealing temperature. Further results showed that relatively shorter annealing duration could induce the apparent changes of crystalline structure and mechanical properties of the PPR sample.

I. INTRODUCTION

The mechanical properties of semicrystalline polymers are greatly dependent upon the processing conditions which determine the supermolecular structures. During the common melt processing procedures including extrusion, injection, and compression, the molecular chains of the semicrystalline polymers are usually in the nonequilibrium state in the viewpiont of thermodynamics. Thus, the molecular chains relax gradually to achieve the thermodynamic equilibrium state during the service period, which induces the changes of the dimension stability and the mechanical properties due to the variations of the supermolecular structures. Annealing treatment, which is carried out at temperatures below the melting point (T_m) of semicrystalline polymers, is one of the efficient ways to accelerate the relaxation of molecular chains and achieve the thermodynamic equilibrium state in a very short time. If the annealing time is long enough, second crystallization of semicrystalline polymer is provoked, leading to the perfection of raw lamellae which are obtained during the common melt processing, and the formation of new thin lamellae in the amorphous region.[1–5] Consequently, physical properties which are greatly dependent upon the supermolecular structures change accordingly. For example, increased tensile modulus, tensile strength, and thermal stability are obtained due to the increased crystallinity and improved crystalline structure induced by annealing treatment.[5–8]

Isotactic polypropylene (iPP) is a typical semicrystalline polymer with complicated supermolecular structures. Although the molecular chains of iPP have enough crystallization ability, the crystallinity of the iPP particles is relatively small under the common melt processing conditions. Thus, annealing is widely used to treat iPP articles so that the microstructure and physical properties can be adjusted to satisfy the requirement. It has been reported that annealing at relatively high temperature promotes not only the transition from the metastable phase to the crystalline phase but also the microstructure rearrangements including lamellae thickening and relaxation of oriented structure.[7,9–11] As a consequence of microstructure rearrangements, the annealed iPP samples usually exhibit enhanced tensile strength and tensile modulus but decreased ductility in comparison with the unannealed samples.[5,12] It is well known to all, the poor impact strength, especially at relatively low temperature, is the main reason which restricts the application of the iPP. Interestingly, it has been widely reported that the impact strength of iPP can be greatly improved by annealing treatment.[13–17] So far, different methods have been developed to evaluate and analyze the effect of annealing treatment on the fracture resistance of iPP.[7,18] For example, some research studies report that the reason for the improvement of impact strength induced by annealing is mainly related to the variation of molecular chain mobility in the amorphous region, which can be proved by the decreased glass transition temperature (T_g) and the enhanced intensity of β-relaxation of the iPP as shown by dynamic mechanical analysis (DMA).[6,13,19] The annealing temperature and the annealing duration are the most important factors which

a)Address all correspondence to this author.
e-mail: yongwang1976@163.com
DOI: 10.1557/jmr.2013.332

 © Materials Research Society 2013

https://doi.org/10.1557/jmr.2013.332 Published online by Cambridge University Press

determine the microstructure rearrangements and physical properties of iPP.[2,14,19–22] For example, it has been proved that annealing at a temperature range of 100–140 °C is favorable for the enhancement of impact strength. The tensile strength and tensile modulus can be greatly increased at relatively higher annealing temperature; however, further enhancing the annealing temperature induces the deterioration of impact strength greatly. Now, annealing treatment is further used to improve the impact strength of the iPP-based composites[5,6,19] or the iPP-based blends.[14,23]

To improve the fracture toughness of PP, other comonomers including ethylene, octene, etc. have been introduced into the polymerization of propylene to obtain the polypropylene random copolymer (PPR) or the polypropylene block copolymer (PPB). The microstructure as well as the mechanical properties of the PPR (or PPB) is greatly dependent upon the amount of comonomer in the material. For example, when PPR has 3 wt% ethylene, the T_m of the PPR is decreased from 160–170 °C of iPP to 140–150 °C.[24] A considerable decrease in crystallinity is observed for metallocene copolymers of propylene-1-hexene and propylene-1-octadecene.[25–29] Specifically, the presence of comonomer endows the molecular chains of the PPR with greater mobility in comparison with that of iPP. It is expected that the enhanced mobility is favorable for the microstructure rearrangements of the PPR during the annealing treatment. Most likely, relatively lower annealing temperature and/or shorter annealing duration is enough to satisfy the requirement of the microstructure rearrangements of the PPR. In the present work, the effects of annealing treatment on the crystalline structure and mechanical property changes of the PPR were mainly investigated.

II. EXPERIMENTAL PART

A. Materials

PPR (3260) was purchased from Total Petrochemical Co. (Paris La Défense Cedex, France). The content of comonomer ethylene is 3 mol%. The melt flow rate is 1.8 g/10 min (230 °C/2.16 kg), and the density is 0.902 g/cm^3.

B. Sample preparation

Before sample preparation, the pellets as obtained were dried at 70 °C for 10 h to erase the effect of moisture. Then, the PPR pellets were directly injection-molded to obtain the standard specimens using an injection-molding machine (EM80-V, China). During the injection-molding process, the melt temperature was 170–180–180 °C from hopper to nozzle and the mold temperature was 25 °C. Subsequently, some specimens were annealed at different temperatures (T_a = 80, 100, 120, and 140 °C, respectively) for 3 h, and the others were annealed at 100 °C for different durations (t_α = 1, 3, 6, and 12 h, respectively). After being annealed, the specimens were cooled in the ambient air and then conditioned at 23 °C and 50% relative humidity for 48 h before testing. The sample notation was defined as PPR-x, where x represented the value of the annealing temperature. For example, PPR-100 indicated that the sample was annealed at 100 °C for 3 h.

C. Wide angle x-ray diffraction

The crystalline structure of PPR was investigated using a wide angle x-ray diffraction (WAXD) X'pert PRO diffractometer (Panalytical, Almelo, Netherlands) with Ni-filtered Cu K_α radiation at 40 kV and 40 mA. It should be stressed that the core zone of the injection-molded bar was characterized so that the effect of preferential orientation on the crystalline structure could be erased as much as possible. The angular range was from 5 to 35°. The X_{c-WAXD} was calculated according to the following relationship:

$$X_{c-WAXD} = \frac{\sum A_{crystalline}}{\sum A_{crystalline} + \sum A_{amorphous}} \times 100\% \quad , \quad (1)$$

where $A_{crystalline}$ and $A_{amorphous}$ are the fitted areas of the diffraction peaks of crystalline and amorphous, respectively.

D. Differential scanning calorimetry

The melting behaviors of samples were investigated by differential scanning calorimetry (DSC STA449C; Netzsch, Selb, Germany). About 8 mg of the sample was directly heated from 30 to 200 °C at a heating rate of 10 °C/min. The degree of crystallinity (X_{c-DSC}) of PPR was calculated according to the following equation:

$$X_{c-DSC} = \frac{\Delta H_m}{\Delta H_m^0} \times 100\% \quad , \quad (2)$$

where ΔH_m is the value of fusion enthalpy of sample obtained during the DSC heating scan, ΔH_m^0 is the fusion enthalpy of the completely crystalline polymer. Here, the ΔH_m^0 of PPR was selected as 207 J/g.[30]

E. Mechanical property measurement

Dynamic mechanical properties of samples were measured using a DMA Q800 (TA Instruments, New Castle, DE). The single cantilever mode was selected, and the measurement was carried out on a rectangular cross-sectional bar (length of 35 mm, width of 10 mm, and thickness of 4 mm) from −60 to 150 °C at a heating rate of 3 °C/min and a frequency of 1 Hz. Three samples were tested repeatedly for each composition and the representative curve was reported. Tensile properties were measured on a universal testing machine AGS-J (SHIMADZU, Shenzhen Reger Instrument Co., Ltd., Shenzhen, China) according to ISO 180/1A at the tensile speed of 50 mm/min.

https://doi.org/10.1557/jmr.2013.332 Published online by Cambridge University Press

Notched Izod impact strength was measured using an impact tester XC-22Z (Chende Jingjian, China) according to ASTM D 256-04. Both tensile and impact measurements were carried out at room temperature. At least five specimens were tested repeatedly, and the average value was reported.

F. Scanning electron microscopy

A scanning electron microscope (SEM) Quanta 200 (FEI, Hillsboro, OR) was used to characterize the impact-fractured surface morphologies of specimens. The accelerating voltage was set at 20 kV. All the samples were sputter-coated with a thin layer of gold prior to SEM characterizations.

III. RESULTS AND DISCUSSION

A. Crystalline structure evolution of PPR during annealing

The crystalline structure evolution of PPR during annealing was first investigated by WAXD, and the results are shown in Fig. 1. For the unannealed PPR sample, the characteristic diffraction peaks at $2\theta = 14.1$, 16.9, 18.6, 21.2, and 21.9° are mainly related to the diffractions of (110), (040), (130), (111), and (041) crystal planes of α-form PP, respectively. Furthermore, one can see an intense characteristic diffraction peak at $2\theta = 20.1°$ attributing to the diffraction of (117) crystal plane of γ-form PP. Factually, it should be also noticed that the diffraction peak at about $2\theta = 14.1°$ is very broad. A shoulder can be differentiated at $2\theta = 13.9°$, which is related to the diffraction of (111) crystal plane of γ-form PP. Generally, formation of γ-form is favored by short isotactic sequences.[31,32] For the PPR used in this work, the counits of ethylene induce the defects in the molecular chains of iPP. Obviously, the defects decrease the isotacticity of iPP, leading to the formation of a large amount of short isotactic sequences. So far, there are many other papers on iPP containing stereodefects and comonomeric unit defects, and the effect of the presence of defects has been explained in terms of average length of regular isotactic sequences for metallocene iPPs and copolymers.[26–29,33–40] According to the methodology developed by Turner-Jones,[41] the relative fraction (K_γ) of γ-form PP can be calculated according to the following equation:

$$K_\gamma = I^\gamma_{(117)} / (I^\gamma_{(117)} + I^\alpha_{(130)}) \quad , \tag{3}$$

where $I^\gamma_{(117)}$ and $I^\alpha_{(130)}$ represent the intensities of the (117) plane of the γ-form and (130) plane of the α-form, respectively. As shown in Table I, X_{c-WAXD} and K_γ of the unannealed PPR sample are 60.0% and 0.68, respectively. For the annealed PPR samples, it can be seen that the variations of crystalline structure are dependent upon the annealing temperature (T_a). At relatively low T_a, both X_{c-WAXD} and K_γ remain nearly invariant. However, for the PPR-140 sample, one can see that the shoulder at $2\theta = 13.9°$ nearly disappeared. Only a single diffraction peak is observed at $2\theta = 14.1°$. Furthermore, one can see that the intensity of the diffraction peak of the (130) crystal plane increased, whereas that of the (117) crystal plane decreased. This suggests a decrease in the amount of γ-form in the sample. According to the variations of X_{c-WAXD} and K_γ as shown in Table I, it can be believed that there is a transition from γ-form to α-form during the annealing treatment at 140 °C.

Figure 2 shows the melting behaviors of the PPR samples with and without annealing treatment. For the unannealed PPR sample, it exhibits a single endothermic peak at 147.0 °C, attributing to the fusion of the α-form. Furthermore, one can see a weak shoulder at about 133.7 °C on the left side of the main endothermic peak. The previous WAXD profiles already prove the presence of the γ-form in the sample. Therefore, it is suggested that the shoulder at 133.7 °C is mainly ascribed to the fusion of the γ-form ($T_{m\gamma}$) as reported in the literature.[42] After being annealed, the PPR-80 sample exhibits another shoulder at relatively lower temperature, i.e., 98.1 °C, indicating the fusion of those thin lamellae which are formed during the annealing process through the second crystallization process. The intensity of the shoulder increases gradually with the enhancement of the T_a, and the position of the shoulder

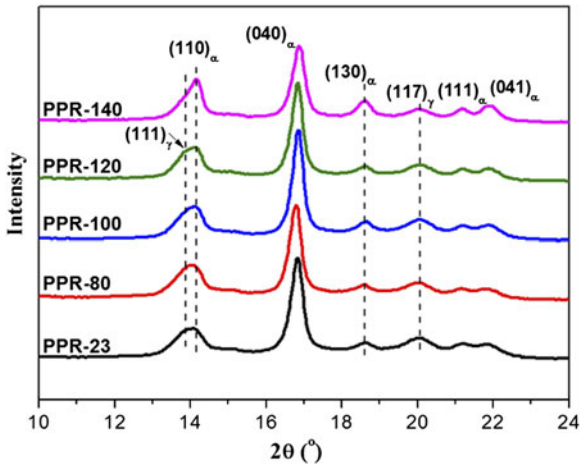


FIG. 1. WAXD profiles show the comparison of crystalline structures of PPR before and after being annealed at different temperatures as indicated in the graph.

TABLE I. The degree of crystallinity and the relative fraction of γ-form PP in different samples. The data were obtained from the WAXD measurement.

Samples	X_{c-WAXD} (%)	K_γ
PPR-23	60.0	0.68
PPR-80	60.8	0.63
PPR-100	62.3	0.62
PPR-120	63.0	0.62
PPR-140	64.9	0.44

https://doi.org/10.1557/jmr.2013.332 Published online by Cambridge University Press

in the DSC curve shifts to higher temperatures as shown in the graph. This indicates the formation of more lamellae with more perfect structure at relatively higher T_a through the second crystallization process. Specifically, for the PPR-120 sample, double endothermic peaks are observed at 137.5 and 148.4 °C. The first endothermic peak at 137.5 °C even exhibits bigger intensity compared with the second one at 148.4 °C. Further enhancing T_a leads to the apparent change of the melting behavior of the PPR-140 sample. First, it exhibits a single endothermic peak at 154.7 °C, indicating the great perfection of crystalline structure in this condition. Obviously, this is mainly attributed to the fusion of α-form with more integrated structure. Second, a very broad endothermic peak is observed at about 131 °C. A similar melting behavior of PPR is observed by Zhao et al.,[43] and they suggested that the broad peak was probably associated with the most ethylene-rich molecular segments induced by the appreciable molecular segregation at relatively high T_a. Here, the previous WAXD measurements show that the PPR-140 sample still has a large number of γ-form and the K_γ is still 0.44. Therefore, it is suggested that both the most ethylene-rich molecular segments and the residual γ-form contribute to the observation of the broad endothermic peak at about 131 °C. The crystallinity was also calculated, and the results further prove the improvement of the crystalline structure in the annealed samples. For example, the X_{c-DSC} of the PPR-100 sample is 29.6%, higher than that of 23.9% of the PPR-23 sample. Further increasing the T_a leads to a slight increase in X_{c-DSC}.

B. Relaxation behavior of annealed PPR

The relaxation behaviors of PPR samples before and after being annealed were investigated using DMA. The mechanical loss factors (tanδ) are shown in Fig. 3, and the corresponding data related to the relaxation behaviors are shown in Table II. From Fig. 3, one can see that the tanδ curve of the unannealed PPR sample exhibits two maxima. The mechanical loss peak at low temperature of 13.1 °C is related to the β-relaxation, which is related to the glass transition of the unrestricted molecular chains of PPR in the amorphous region. The peak at 73.2 °C is mainly related to α_c-relaxation, which mainly originated from the relaxation of restricted molecular chains of PPR in the crystalline phase with defects, also known as the rigid fraction.[44–46] Then, the temperature relating to the β-relaxation peak is defined as the T_g of the sample. As shown in Table II, the annealed PPR samples exhibit much smaller T_g compared with the unannealed one. For example, the T_g of the PPR-80 sample is 9.4 °C, which is apparently smaller than 13.1 °C of the unannealed one. This indicates the enhancement of molecular chain mobility in the amorphous region of the annealed PPR sample. In addition, one can see that further increasing the T_a does not induce the further decrease of the T_g apparently. This is different from the influence of the annealing temperature on the T_g of the iPP sample, in which the T_g decreases gradually with the increase of the T_a[13,19,23] The intensity of the $\tan\delta_{max}$ and the integration area of the β-relaxation (I_R) are also shown in Table II. It can be seen that, although annealing treatment does not induce the

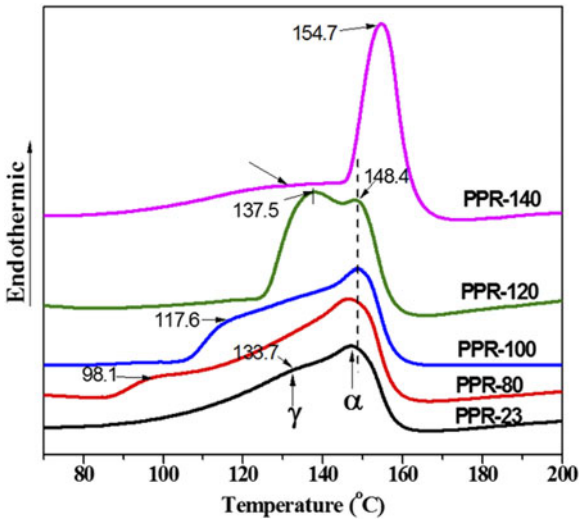


FIG. 2. DSC heating curves show the melting behaviors of PPR before and after being annealed at different temperatures for 3 h as indicated in the graph.

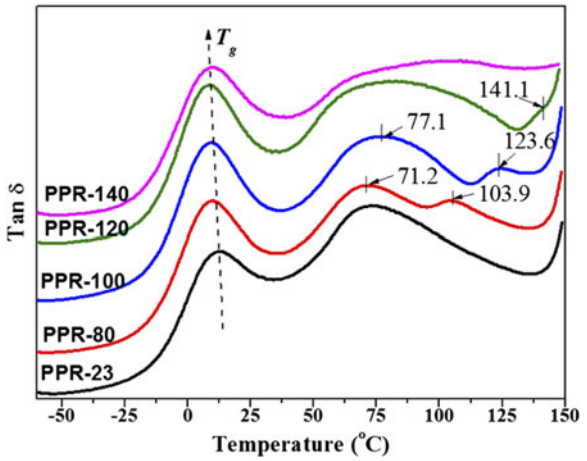


FIG. 3. Mechanical loss factor (tanδ) of PPR before and after being annealed at different temperatures for 3 h as indicated in the graph.

TABLE II. β-relaxation parameters obtained from DMA measurement for the PPR sample with and without annealing treatment.

Samples	T_g (°C)	$\tan\delta_{max}$	Integration
PPR-23	13.13	0.09	0.079
PPR-80	9.37	0.09	1.05
PPR-100	9.22	0.10	1.29
PPR-120	8.52	0.09	1.25
PPR-140	8.97	0.09	1.25

https://doi.org/10.1557/jmr.2013.332 Published online by Cambridge University Press

apparent change of the intensity of $\tan\delta_{max}$, the I_R of the annealed sample is greatly increased in comparison with that of the unannealed sample. This represents that more energy is dissipated because of the viscoelastic relaxation of the PPR. It has been proved in the literature that there is a certain relationship between the I_R and the impact strength of the samples.[47] Namely, if the sample has excellent impact strength in the mechanical measurement, it usually has bigger I_R during the DMA measurement. This indicates that the annealed PPR sample most likely exhibits higher impact strength compared with the unannealed one.

In addition, one can also see that annealing treatment promotes the change of the relaxation behaviors of molecular chains in the defect of the crystalline region of the annealed PPR samples. For the PPR-80 sample, double α_c-relaxation peaks are observed at 71.2 and 103.9 °C, indicating that the molecular chains in the defect of the crystalline region exhibit at least two different states. With an increase in the T_a, the two α_c-relaxation peaks shift to higher temperatures, indicating the increased degree of the restriction of molecular chains. This also indicates indirectly the perfection of the crystalline structure at relatively high T_a. However, for the PPR-140 sample, a single broad α_c-relaxation peak is observed again. Both the intensity and the integration area of the relaxation peak are greatly decreased in comparison with those of the unannealed sample, indicating the decreased rigid fraction in the crystalline region. The similar relaxation behavior with several transitions has been found for metallocene copolymers of propylene-1-hexene and propylene-1-octadecene,[25] especially, the location and intensity of the transitions are strongly dependent upon the composition. Here, annealing treatment does not induce the change of the composition but induce the perfection of the crystalline structure. Considering the presence of both α-form and γ-form in the sample, it is speculated that the double α_c-relaxation peaks are possibly related to the different relaxation behaviors of molecular chains in the different crystals. Further work needs to be done to understand the annealing treatment on the α_c-relaxation of the PPR sample.

C. Mechanical properties

The tensile properties of the unannealed and annealed PPR samples were first measured, and the results are shown in Fig. 4. Figure 4(a) shows the representative stress–strain curves of the different samples, and the corresponding mechanical properties are shown in Fig. 4(b). As shown in Fig. 4(a), the typical stress–strain curve of the semicrystalline polymer is observed for the unannealed PPR sample. The stress–strian curve can be subclassified into several regions, representing the different stages of the sample during the tensile measurement: (i) the elastic region (linear increase in stress with strain), (ii) yield point (maximum yield stress obtained in the stress–strain curve), (iii) stress drop region (dramatic decrease in stress with almost invariant strain), (iv) cold-drawing region (almost invariant stress with strain, relating to the orientation of molecular chains in the amorphous region and the slippage and orientation of lamellae in the crystalline region along the tensile direction), and (v) fracture point. For the annealed PPR sample, there are at least two features which can be observed from the stress–strain curves. First, the cold-drawing region is largely decreased and even disappears completely at relatively high T_a. Second, the stress-drop phenomenon also becomes inconspicuous. Similar phenomena have been observed for the annealed iPP and its blends, and the reason is mainly attributed to the removing of the structure discrepancy during the annealing treatment.[5,14] As is well known, the stress-drop phenomenon is mainly related to the nucleation and propagation of some microvoids during the tensile process. This indicates that the annealed PPR sample has more homogeneous crystalline structures and fewer defects, and the stress transfer becomes easier during the universal tensile process. As shown in Fig. 4(b), the unannealed PPR sample exhibits excellent ductility with elongation at break (%) bigger than 450%. After being annealed, largely decreased ductility is observed for all the annealed samples. Specifically, the higher the T_a, the smaller the ductility is. For example, the PPR-140 sample exhibits an elongation at break (%) of 21.8%, which is much smaller than that of the unannealed PPR sample. The decrease in the ductility is mainly ascribed to the increase of the crystallinity and the improvement of the crystalline structure as shown by previous WAXD and DSC measurements on one hand. On the other hand, the formation of new α-form with more integrated structure, which is induced through the transition from γ-form to α-form at relatively high T_a, possibly contributes to the large decrease of the ductility. In addition, although the tensile modulus is not influenced apparently, the tensile strength of the annealed samples is higher than that of the unannealed one.

Figure 5 exhibits the variation of the notched Izod impact strength of PPR samples versus the annealing temperature. The unannealed PPR sample exhibits an impact strength of 7.2 kJ/m^2. After being annealed, the annealed samples exhibit largely increased impact strength. The degree of the enhancement of the impact strength is dependent upon the T_a. For example, at an T_a of 100 °C, the impact strength is increased up to 19.5 kJ/m^2, more than two times higher than that of the unannealed sample. The PPR-120 sample exhibits a similar impact strength to that of the PPR-100 sample. However, further increasing T_a leads to the decrease of the impact strength. Considering the variations of both impact strength and tensile properties, it is suggested that 100 °C is possibly the most appropriate temperature for achieving PPR sample with excellent comprehensive mechanical properties. It has been reported that for the annealed iPP and its blends, the appropriate annealing temperatures are in the

https://doi.org/10.1557/jmr.2013.332 Published online by Cambridge University Press

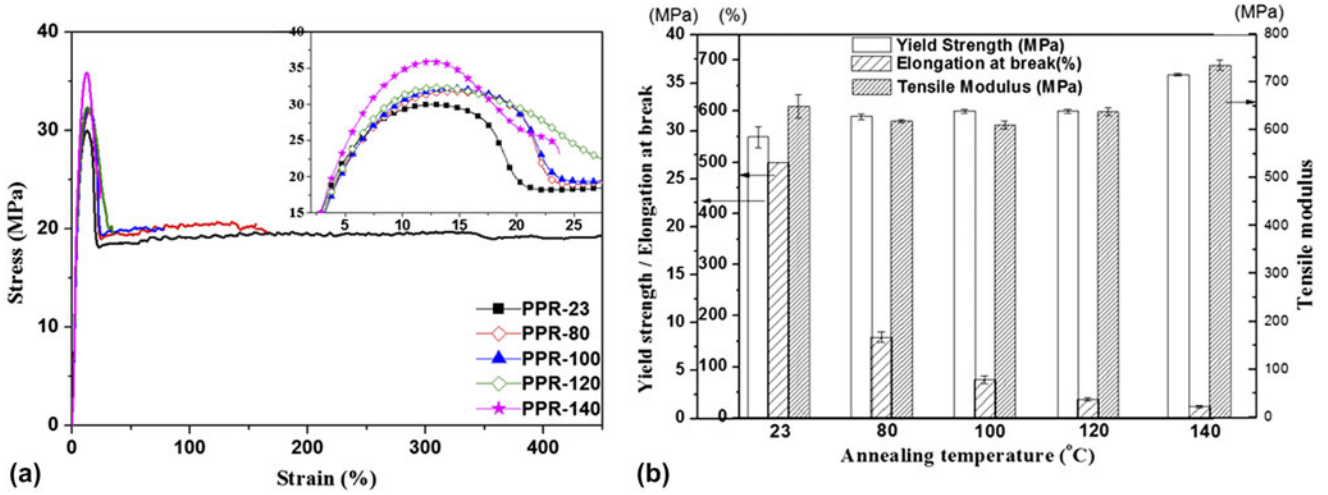


FIG. 4. (a) The typical stress–strain curves of PPR samples obtained before and after being annealed at different temperatures for 3 h as indicated in the graph, (b) the corresponding tensile properties obtained from the tensile measurement.

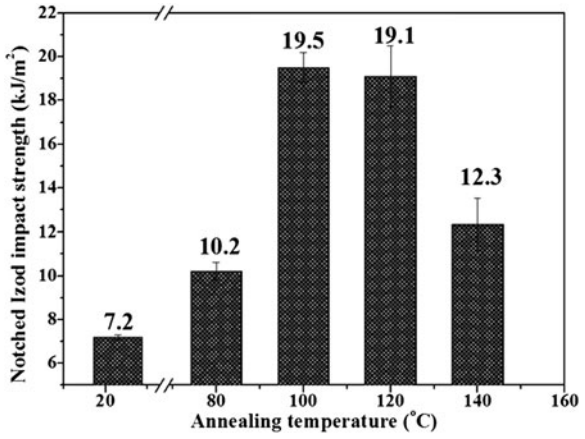


FIG. 5. Variation of the notched Izod impact strength of PPR versus the annealing temperature.

range of 120–140 °C.[14] Obviously, the difference between the appropriate temperatures of PPR and iPP is mainly due to the different molecular chain mobilities and crystalline structures of the samples. As shown by DMA measurement, the presence of ethylene counits enhances the chain mobility greatly accompanied by a great decrease of T_g in comparison with that of iPP. This promotes the occurrence of the molecular chain rearrangement at relatively low T_a.

To further understand the influence of annealing on the fracture behavior of PPR, the impact-fractured surface morphologies of the unannealed and annealed PPR-100 samples were characterized using SEM, and the results are shown in Fig. 6. From Fig. 6, it can be seen that at small magnification, there are several differences between the surface morphologies of the PPR-23 and the PPR-100 samples. First, the impact-fractured surface of the annealed PPR-100 sample is rougher than that of the PPR-23 sample, which indicates that more energy absorption during the fracture process. Second, although a small zone with parabolic ridge or a thin curved band relating to the change in the stress state is also observed for the PPR-23 and PPR-100 sample, the location of the parabolic ridge in the surface is different. Namely, the parabolic ridge of the PPR-100 sample shifts to the right side in comparsion with that of the PPR-23 sample. Furthermore, it can be seen that there is an apparent core zone with bulge morphology in the impact-fractured surface of the annealed PPR-100 sample. Generally, during the impact testing, the plane strain state prevails during the impact fracture of the sample and the plane stress state prevails only in the skin of the sample. From Fig. 6, a slightly serrated surface can be differentiated in the skin of the annealed PPR-100 sample. This is different from the smooth surface of the PPR-23 sample in the skin region, indicating that annealing treatment amplifies the role of the plane stress state during the impact measurement of the annealed sample.

Generally speaking, the fracture of the sample under the load conditions includes crack initiation and crack propagation processes. Herein, the surface morphologies in different zones of the fractured surface were carefully characterized at high magnification. The results are also shown in Fig. 6. It can be seen that in the crack initiation zone, the PPR-23 sample [Fig. 6(a1)] exhibits relatively smooth surface, whereas the local plastic deformation is observed for the PPR-100 sample [Fig. 6(b1)]. Furthermore, whether in the early stage or in the later stage of the crack propagation zone [from zone 2 to zone 4 as indicated in the Fig. 6(a) and/or Fig. 6(b)], one can see that the PPR-100 sample exhibits apparent plastic deformation phenomenon, which may be the main reason for the largely enhanced impact strength of the PPR-100 sample in comparison with that of the PPR-23 sample. Since the plastic deformation ability of the sample is mainly determined by the molecular chain mobility, it is suggested that the enhanced chain mobility in the amorphous region, which is realized through

https://doi.org/10.1557/jmr.2013.332 Published online by Cambridge University Press

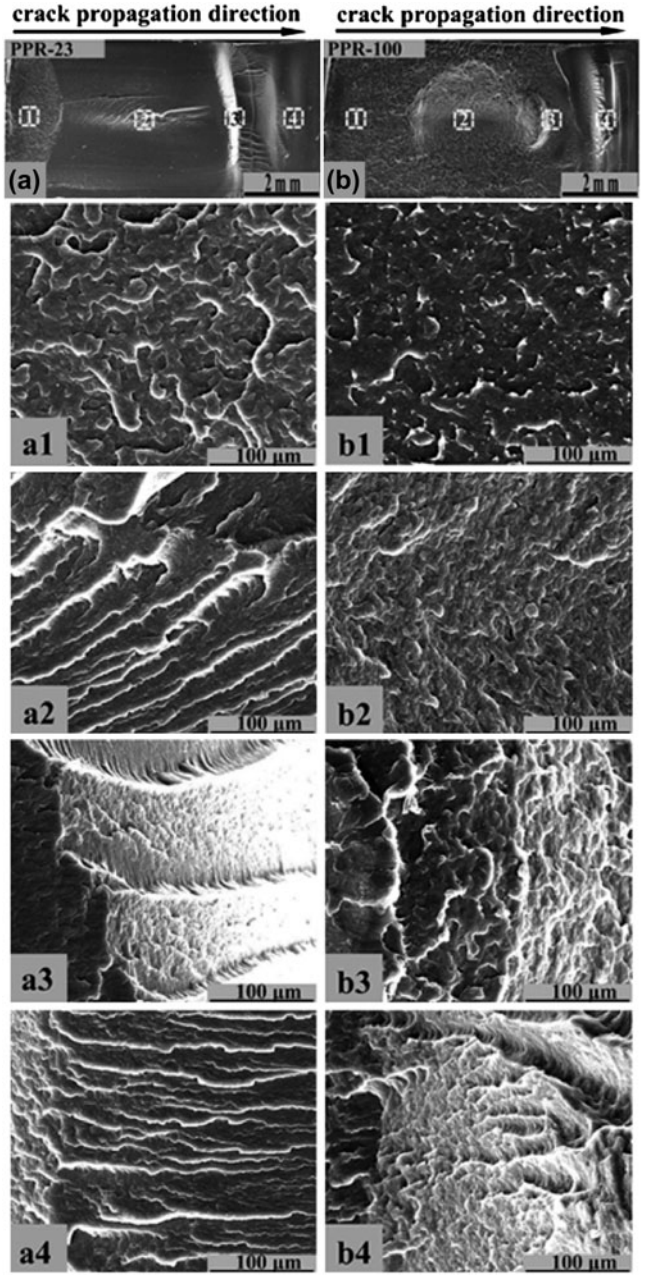


FIG. 6. SEM images show the impact-fractured surface morphologies of (a) unannealed PPR-23 and (b) annealed PPR-100 samples. (a) and (b) show the morphologies observed at relatively small magnification. (a1–a4) and (b1–b4) show the morphologies observed at relatively big magnification, corresponding to the different zones as indicated in images (a) and (b), respectively.

annealing treatment, is the main reason for the largely increased impact strength.

D. Effect of annealing duration on the crystalline structure evolution and impact strength

In this part, the effect of annealing duration (t_a) on the crystalline structure evolution was characterized using DSC, and the results are shown in Fig. 7. From Fig. 7,

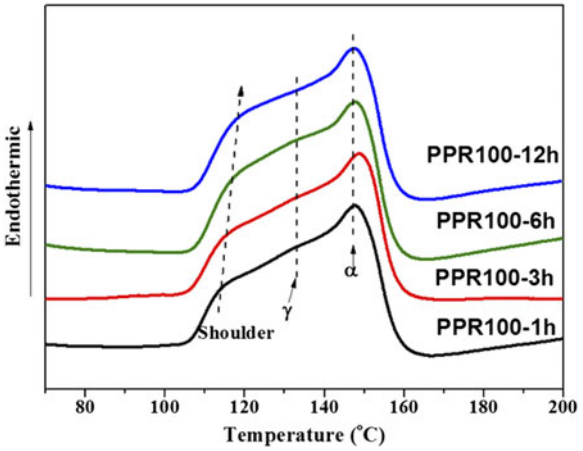


FIG. 7. DSC heating curves show the melting behaviors of PPR-100 samples after being annealed for different durations.

one can see that even if the t_a is only 1 h, the annealed PPR-100 sample exhibits apparently different melting behaviors in comparison with the unannealed PPR as shown in Fig. 2. Further increasing the t_a only induces the shift of shoulder from about 114.1 to 118.8 °C. This indicates that prolonging annealing duration facilitates the occurrence of the second crystallization process during the annealing treatment. However, nearly invariant $T_{m\gamma}$ and $T_{m\alpha}$ are observed, even if the t_a is increased up to 12 h. This indicates that annealing treatment at relatively low temperature (herein, 100 °C) does not induce an apparent change in the already existing crystalline structure but induces the apparent change of the new lamellae formed during the annealing process. Namely, longer t_a facilitates the perfection of a new lamellar structure rather than the lamellar thickening of the primary crystallites. Interestingly, it is observed that the effect of the t_a on the X_{c-DSC} is inconspicuous, and all the samples exhibit similar X_{c-DSC}. For example, at an t_a of 1 h, the X_{c-DSC} is increased up to 29.4%, which is similar to 29.6% of the sample obtained after being annealed for 3 h. This further indicates that the crystalline structure rearrangement of the PPR sample can be achieved in a very short annealing duration.

The notched Izod impact strength of the annealed PPR-100 obtained at different t_a was also measured, and the results are shown in Fig. 8. For making a comparison, the impact strength of the PPR-23 sample was also shown in the graph. It can be seen that after being annealed for only 1 h, the annealed PPR-100 sample exhibits largely increased impact strength. The impact strength is increased up to 11.2 kJ/m^2, which is about 55.6% higher than that of the unannealed PPR sample. When the t_a is increased up to 3 h, the impact strength is further increased up to 19.5 kJ/m^2. However, further increasing the t_a does not insure the further enhancement of the impact strength. The previous results show that at an t_a of 3 h, the annealed PPR-120 sample exhibits a similar impact strength to that

https://doi.org/10.1557/jmr.2013.332 Published online by Cambridge University Press

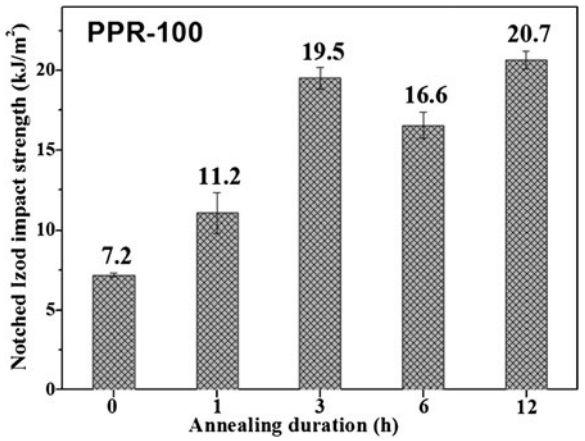


FIG. 8. Variation of the notched Izod impact strength of PPR-100 samples versus the annealing duration.

of the PPR-100 sample. Here, the t_a is increased from 3 to 12 h; however, the annealed samples still show similar impact strengths. This indicates that the annealing duration of 3 h is enough to obtain the annealed sample with excellent impact strength. This is also different from the effect of the t_a on the impact strength of iPP sample, in which the impact strength increases gradually with increasing t_a.[6,14] Obviously, the largely enhanced molecular chain mobility of PPR induced by the presence ethylene counites in the main chain is the main reason for the crystalline structure rearrangement in a very short time during the annealing process. In other words, the toughening efficiency of annealing treatment on the PPR sample is higher than that on the iPP sample.

IV. CONCLUSIONS

In summary, the effects of the annealing treatment on the crystalline structure and mechanical properties of the PPR have been investigated. Both WAXD and DSC measurements show that annealing treatment promotes the perfection of the crystalline structure at a relatively low annealing temperature below 120 °C. At annealing temperature higher than 140 °C, a transition from γ-form to α-form is detected. Largely enhanced chain mobility is achieved for the annealed PPR samples as proved by DMA measurements. As a consequence, annealed PPR samples exhibit much bigger impact strength in comparison with that of the unannealed PPR sample. Further results show that the crystalline structure rearrangements of the PPR sample can be achieved in a very short annealing duration. Further increasing the annealing duration does not change the crystalline structure and mechanical properties apparently.

ACKNOWLEDGMENTS

Authors express their sincere thanks to the National Natural Science Foundation of China (Grant No. 51173151), Distinguished Young Scholars Foundation of Sichuan (Grant No. 2012JQ0057), and the Fundamental Research Funds for the Central Universities (Grant Nos. SWJTU12CX010, SWJTU11CX142, and SWJTU11ZT10) for financial support. Prof. Qiang Fu (Sichuan University, People's Republic of China) is greatly appreciated for the assistance of the DMA measurement.

REFERENCES

1. P. Maiti, M. Hikosaka, K. Yamada, A. Toda, and F. Gu: Lamellar thickening in isotactic polypropylene with high tacticity crystallized at high temperature. *Macromolecules* **33**, 9069 (2000).
2. A.D. Drozdov and J. deClaville Christiansen: The effect of annealing on the time-dependent behavior of isotactic polypropylene at finite strains. *Polymer* **43**, 4745 (2002).
3. J. Zhao, J. Qiu, Y. Niu, and Z. Wang: Evolutions of morphology and crystalline ordering upon annealing of quenched isotactic polypropylene. *J. Polym. Sci. Polym. Phys.* **47**, 1703 (2009).
4. C. Hedesiu, D. Demco, R. Kleppinger, G.V. Poel, W. Gijsbers, B. Blümich, K. Remerie, and V. Litvinov: Effect of temperature and annealing on the phase composition, molecular mobility, and the thickness of domains in isotactic polypropylene studied by proton solid-state NMR, SAXS, and DSC. *Macromolecules* **40**, 3977 (2007).
5. H. Wu, X. Li, J. Chen, L. Shao, T. Huang, Y. Shi, and Y. Wang: Reinforcement and toughening of polypropylene/organic montmorillonite nanocomposite using β-nucleating agent and annealing. *Composites Part B: Eng.* **44**, 439 (2013).
6. L. Han, X. Li, Y. Li, T. Huang, Y. Wang, J. Wu, and F. Xiang: Influence of annealing on microstructure and physical properties of isotactic polypropylene/calcium carbonate composites with β-phase nucleating agent. *Mater. Sci. Eng., A* **527**, 3176 (2010).
7. D. Ferrer-Balas, M.L. Maspoch, A. Martinez, and O. Santana: Influence of annealing on the microstructural, tensile and fracture properties of polypropylene films. *Polymer* **42**, 1697 (2001).
8. S. Song, J. Feng, and P. Wu: Annealing of melt-crystallized polyethylene and its influence on microstructure and mechanical properties: A comparative study on branched and linear polyethylenes. *J. Polym. Sci. Polym. Phys.* **49**, 1347 (2011).
9. H. Wu, X. Li, F. Xiang, T. Huang, Y. Shi, and Y. Wang: Microstructure evolution of isotactic polypropylene during annealing: Effect of poly(ethylene oxide). *Chin. J. Polym. Sci.* **30**, 199 (2012).
10. C. De Rosa, O. Ruiz de Ballesteros, F. Auriemma, and R. Savarese: Polymorphic transitions induced by annealing in stretched fibers of syndiotactic polypropylene. *Macromolecules* **38**, 4791 (2005).
11. S. Song, J. Feng, and P. Wu: Relaxation of shear-enhanced crystallization in impact-resistant polypropylene copolymer: Insight from morphological evolution upon thermal treatment. *Polymer* **51**, 5267 (2010).
12. H. Bai, F. Luo, T. Zhou, H. Deng, K. Wang, and Q. Fu: New insight on the annealing induced microstructural changes and their roles in the toughening of β-form polypropylene. *Polymer* **52**, 2351 (2011).
13. J.W. Chen, J. Dai, J.H. Yang, N. Zhang, T. Huang, and Y. Wang: Enhancing chain segments mobility to improve the fracture toughness of polypropylene. *Chin. J. Polym. Sci.* **31**, 232 (2013).
14. H. Wu, X. Li, Y. Wang, J. Wu, T. Huang, and Y. Wang: Fracture behaviors of isotactic polypropylene/poly(ethylene oxide) blends: Effect of annealing. *Mater. Sci. Eng., A* **528**, 8013 (2011).
15. Y. Lin, H. Chen, C.M. Chan, and J. Wu: High impact toughness polypropylene/$CaCO_3$ nanocomposites and the toughening mechanism. *Macromolecules* **41**, 9204 (2008).

https://doi.org/10.1557/jmr.2013.332 Published online by Cambridge University Press

16. Y. Lin, H. Chen, C.M. Chan, and J. Wu: Annealing-induced high impact toughness of polypropylene/$CaCO_3$ nanocomposites. *J. Appl. Polym. Sci.* **124**, 77 (2012).
17. B. Na, Z. Li, R. Lv, and S. Zou: Annealing-induced structural rearrangement and its toughening effect in injection-molded isotactic polypropylene. *Polym. Eng. Sci.* **52**, 893 (2012).
18. Q.G. Li, B.H. Xie, W. Yang, Z.M. Li, W.Q. Zhang, and M.B. Yang: Effect of annealing on fracture behavior of poly(propylene-block-ethylene) using essential work of fracture analysis. *J. Appl. Polym. Sci.* **103**, 3438 (2007).
19. H. Bai, Y. Wang, Z. Zhang, L. Han, Y. Li, L. Liu, Z. Zhou, and Y. Men: Influence of annealing on microstructure and mechanical properties of isotactic polypropylene with β-phase nucleating agent. *Macromolecules* **42**, 6647 (2009).
20. A.D. Drozdov: The effect of annealing on the elastoplastic response of isotactic polypropylene. *Eur. Polym. J.* **39**, 21 (2003).
21. A.D. Drozdov and J.D. Christiansen: The effect of annealing on the nonlinear viscoelastic response of isotactic polypropylene. *Polym. Eng. Sci.* **43**, 946 (2003).
22. P. Frontini and A. Fave: The effect of annealing temperature on the fracture performance of isotactic polypropylene. *J. Mater. Sci.* **30**, 2446 (1995).
23. X. Li, H. Wu, L. Han, T. Huang, Y. Wang, H. Bai, and Z. Zhou: Annealing induced microstructure and fracture resistance changes in isotactic polypropylene/ethylene-octene copolymer blends with and without β-phase nucleating agent. *J. Polym. Sci. Polym. Phys.* **48**, 2108 (2010).
24. J. Tang, W. Tang, H. Yuan, and R. Jin: Super-toughed polymer blends derived from polypropylene random copolymer and ethylene/styrene interpolymer. *J. Appl. Polym. Sci.* **115**, 190 (2010).
25. H. Palza, J.M. López-Majada, R. Quijada, J.M. Pereña, R. Benaventa, E. Pérez, and M.L. Cerrada: Comonomer length influence on the structure and mechanical response of metallocenic polypropyleneic materials. *Macromol. Chem. Phys.* **209**, 2259 (2008).
26. C. De Rosa, S. Dello Iacono, F. Auriemma, E. Ciaccia, and L. Resconi: Physical aging of single wall carbon nanotube polymer nanocomposites: Effect of functionalization of the nanotube on the enthalpy relaxation. *Macromolecules* **39**, 6098 (2006).
27. C. De Rosa, F. Auriemma, O.R.D. Ballesteros, D.D. Luca, and L. Resconi: The double role of comonomers on the crystallization behavior of isotactic polypropylene: Propylene-hexene copolymers. *Macromolecules* **41**, 2172 (2008).
28. C. De Rosa, F. Auriemma, O. Ruiz de Ballesteros, S. Dello Iacono, D. De Luca, and L. Resconi: Stress-induced polymorphic transformations and mechanical properties of isotactic propylene-hexene copolymers. *Cryst. Growth Des.* **9**, 165 (2009).
29. C. De Rosa, F. Auriemma, R. Di Girolamo, L. Romano, and M.R. De Luca: New mesophase of isotactic polypropylene in copolymers of propylene with long branched comonomers. *Macromolecules* **43**, 8559 (2010).
30. H.S. Bu and S.Z.D. Cheng, and B. Wunderlich: Addendum to the thermal properties of polypropylene. *Makromol. Chem. Rapid Commun.* **9**, 75 (1988).
31. D. Morrow and B. Newman: Crystallization of low-molecular-weight polypropylene fractions. *J. Appl. Phys.* **39**, 4944 (1968).
32. E. Addink and J. Beintema: Polymorphism of crystalline polypropylene. *Polymer* **2**, 185 (1961).
33. I. Hosier, R. Alamo, P. Esteso, J. Isasi, and L. Mandelkern: Formation of the α and γ polymorphs in random metallocene-propylene copolymers: Effect of concentration and type of comonomer. *Macromolecules* **36**, 5623 (2003).
34. C. De Rosa, F. Auriemma, A. Di Capua, L. Resconi, S. Guidotti, I. Camurati, I.E. Nifant'ev, and I.P. Laishevtsev: Structure-property correlations in polypropylene from metallocene catalysts: Stereodefective, regioregular isotactic polypropylene. *J. Am. Chem. Soc.* **126**, 17040 (2004).
35. C. De Rosa and F. Auriemma: Structural-mechanical phase diagram of isotactic polypropylene. *J. Am. Chem. Soc.* **128**, 11024 (2006).
36. C. De Rosa, F. Auriemma, and T. Circelli: Crystallization of the α and γ forms of isotactic polypropylene as a tool to test the degree of segregation of defects in the polymer chains. *Macromolecules* **35**, 3622 (2002).
37 F. Auriemma and C.D. Rosa: Crystallization of metallocene-made isotactic polypropylene: Disordered modifications intermediate between the α and γ forms. *Macromolecules* **35**, 9057 (2002).
38. C. De Rosa, F. Auriemma, C. Spera, G. Talarico, and O. Tarallo: Comparison between polymorphic behaviors of Ziegler-Natta and metallocene-made isotactic polypropylene: The role of the distribution of defects in the polymer chains. *Macromolecules* **37**, 1441 (2004).
39. C. De Rosa, F. Auriemma, O. Ruiz de Ballesteros, L. Resconi, and I. Camurati: Tailoring the physical properties of isotactic polypropylene through incorporation of comonomers and the precise control of stereo- and regioregularity by metallocene catalysts. *Chem. Mater.* **19**, 5122 (2007).
40. C. De Rosa, F. Auriemma, O. Ruiz de Ballesteros, L. Resconi, and I. Camurati: Crystallization behavior of isotactic propylene–ethylene and propylene–butene copolymers: Effect of comonomers versus stereodefects on crystallization properties of isotactic polypropylene. *Macromolecules* **40**, 6600 (2007).
41. A. Turner-Jones: Development of the γ-crystal form in random copolymers of propylene and their analysis by DSC and x-ray methods. *Polymer* **12**, 487 (1971).
42. Q. Shi, C.L. Cai, Z. Ke, L.G. Yin, Y.L. Liu, L.C. Zhu, and J.H. Yin: Effect of the nucleating agent 1,3:2,4-di(3,4-dimethylbenzylidene) sorbitol on the γ-phase content of propylene/ethylene copolymer. *Eur. Polym. J.* **44**, 2385 (2008).
43. Y. Zhao, A. Vaughan, S. Sutton, and S. Swingler: On the crystallization, morphology and physical properties of a clarified propylene/ethylene copolymer. *Polymer* **42**, 6587 (2001).
44. H. Xu and P. Cebe: Heat capacity study of isotactic polystyrene: Dual reversible crystal melting and relaxation of rigid amorphous fraction. *Macromolecules* **37**, 2797 (2004).
45. S.H. Lu and P. Cebe: The effects of annealing on the disappearance and creation of constrained amorphous phase. *Polymer* **37**, 4857 (1996).
46. M. Song: Rigid amorphous phase and low temperature melting endotherm of poly(ethylene terephthalate) studied by modulated differential scanning calorimetry. *J. Appl. Polym. Sci.* **81**, 2779 (2001).
47. C. Grein, K. Bernreitner, and M. Gahleitner: Potential and limits of dynamic mechanical analysis as a tool for fracture resistance evaluation of isotactic polypropylenes and their polyolefin blends. *J. Appl. Polym. Sci.* **93**, 1854 (2004).

https://doi.org/10.1557/jmr.2013.332 Published online by Cambridge University Press